Report

Cell Reports

Functional Dominance of CHIP-Mutated Hematopoietic Stem Cells in Patients Undergoing Autologous Transplantation

Graphical Abstract

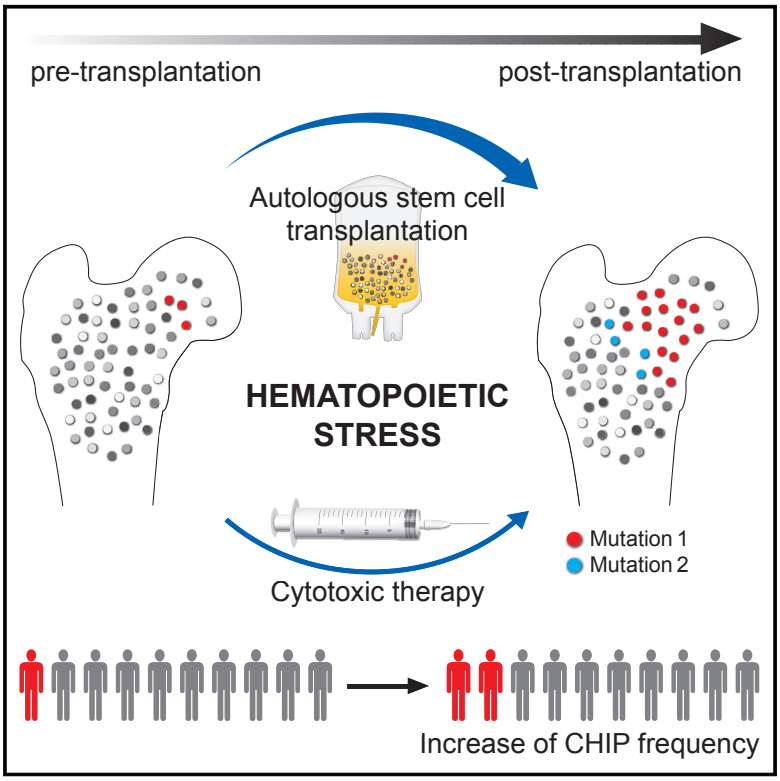

Highlights

- Autologous stem cell transplantation promotes the expansion of mutant blood clones
- CHIP-mutated human stem cells engraft long term and dominate blood reconstitution
- Neutrophil reconstitution post-transplantation is delayed in patients with CHIP

Authors

Christina A. Ortmann, Lena Dorsheimer, Khalil Abou-El-Ardat, ..., Sebastian Wagner, Hubert Serve, Michael A. Rieger

Correspondence

m.rieger@em.uni-frankfurt.de

In Brief

With age, human hematopoiesis becomes affected by blood cell clones with recurrent acquired mutations, resulting in clonal hematopoiesis (CHIP). Ortmann et al. show that hematopoietic stress caused by autologous stem cell transplantation and cytotoxic therapy promotes both size and number of mutant clones in 81 myeloma and lymphoma patients.

Ortmann et al., 2019, Cell Reports 27, 2022–2028
May 14, 2019
https://doi.org/10.1016/j.celrep.2019.04.064

CellPress

OPEN ACCESS
CellPress

Cell Reports
Report

Functional Dominance of CHIP-Mutated Hematopoietic Stem Cells in Patients Undergoing Autologous Transplantation

Christina A. Ortmann,[1] Lena Dorsheimer,[1] Khalil Abou-El-Ardat,[1,2] Jennifer Hoffrichter,[1] Birgit Assmus,[3] Halvard Bonig,[4] Anica Scholz,[5] Heike Pfeifer,[1] Hans Martin,[1] Tobias Schmid,[5] Bernhard Brüne,[5] Sebastian Scheich,[1] Björn Steffen,[1] Julia Riemann,[1] Stella Hermann,[6] Alexandra Dukat,[1,6] Gesine Bug,[1] Christian H. Brandts,[1,2,7] Sebastian Wagner,[1,2] Hubert Serve,[1,2] and Michael A. Rieger[1,2,8,*]

[1]Department of Medicine II, Hematology/Oncology, Goethe University Hospital, Frankfurt am Main 60590, Germany
[2]German Cancer Consortium (DKTK) and German Cancer Research Center (DKFZ), Heidelberg 69120, Germany
[3]Department of Medicine, Cardiology, Goethe University Hospital, Frankfurt am Main 60590, Germany
[4]Institute for Transfusion Medicine and Immunohematology of Goethe University and German Red Cross Blood Service BaWüHe, Frankfurt am Main 60528, Germany
[5]Institute for Biochemistry I, Faculty of Medicine, Goethe University, Frankfurt am Main 60528, Germany
[6]Ambulantes Krebszentrum Schaubstrasse (AKS), Frankfurt am Main 60596, Germany
[7]University Cancer Center Frankfurt (UCT), Goethe University Hospital, Frankfurt am Main 60590, Germany
[8]Lead Contact
*Correspondence: m.rieger@em.uni-frankfurt.de
https://doi.org/10.1016/j.celrep.2019.04.064

SUMMARY

Clonal hematopoiesis of indeterminate potential (CHIP) is caused by recurrent somatic mutations leading to clonal blood cell expansion. However, direct evidence of the fitness of CHIP-mutated human hematopoietic stem cells (HSCs) in blood reconstitution is lacking. Because myeloablative treatment and transplantation enforce stress on HSCs, we followed 81 patients with solid tumors or lymphoid diseases undergoing autologous stem cell transplantation (ASCT) for the development of CHIP. We found a high incidence of CHIP (22%) after ASCT with a high mean variant allele frequency (VAF) of 10.7%. Most mutations were already present in the graft, albeit at lower VAFs, demonstrating a selective reconstitution advantage of mutated HSCs after ASCT. However, patients with CHIP mutations in DNA-damage response genes showed delayed neutrophil reconstitution. Thus, CHIP-mutated stem and progenitor cells largely gain on clone size upon ASCT-related blood reconstitution, leading to an increased future risk of CHIP-associated complications.

INTRODUCTION

Hematopoiesis is maintained by a highly polyclonal production of all mature blood cells (Sun et al., 2014; Pei et al., 2017; Yu et al., 2018). Exome sequencing revealed single recurrent somatic mutations in myeloid malignancy-related genes, most predominantly in the genes *DNMT3A*, *TET2*, and *ASXL1*, that cause the emergence of expanded blood cell clones (Genovese et al., 2014; Jaiswal et al., 2014; Xie et al., 2014; McKerrell et al., 2015). This phenomenon has been called clonal hematopoiesis of indeterminate potential (CHIP) (Steensma et al., 2015), because despite oligoclonality, no obvious hematologic abnormalities were detectable in these people. However, CHIP increases with age and is associated with increased overall mortality, increased risk for cardiovascular diseases, and a higher propensity to develop into myeloid neoplasms (Steensma et al., 2015; Jaiswal et al., 2017; Dorsheimer et al., 2019). The presence of CHIP in cancer patients correlates with the emergence of treatment-induced secondary myeloid neoplasms (Gillis et al., 2017; Takahashi et al., 2017).

Little is known about the development of CHIP-mutated clones in individuals over time. A retrospective study revealed that the mutated clone was stable for more than 10 years under homeostatic hematopoiesis in healthy women (Young et al., 2016). However, steady-state hematopoiesis is largely maintained at the progenitor level, and hematopoietic stem cells (HSCs) are deeply quiescent (Wilson et al., 2008; Sun et al., 2014; Cabezas-Wallscheid et al., 2017). In contrast, stress hematopoiesis relies on the reactivation of HSCs. Stress is induced by cytotoxic therapy, chronic infections, blood loss (Walter et al., 2015), and in particular, myeloablative regimens and subsequent stem cell transplantation. This procedure demands several features of HSCs: first, they need to successfully implant into the bone marrow; second, they must expand and establish the hematopoietic stem and progenitor cell pool; and finally, they provide the life-long self-renewing pool of HSCs (Eaves, 2015).

In this study, we addressed in a patient cohort receiving autologous stem cell transplantation (ASCT) how hematologic stress affects the development of CHIP, whether HSCs carrying CHIP mutations are able to reconstitute the blood system, and whether they outcompete non-mutated HSCs upon transplantation by clonal dominance. We took advantage of the fact that upon transplantation, only long-term repopulating HSCs (LT-HSCs) can reconstitute the patient over long periods. All mature blood cells several months to years after transplantation

Table 1. Baseline Characteristics of Patient Cohort according to CHIP Status in Post-transplantation Blood Sample

Attribute	Total Cohort (n = 81)	CHIP Positive in Blood (n = 18)	CHIP Negative in Blood (n = 63)	p Value (CHIP Positive versus Negative)
Age at cancer diagnosis (years)	53.9 ± 11.4	60.7 ± 5.5	52.0 ± 11.9	0.004*
	56.0 (47.0; 63.0)	60.0 (58.3; 65.0)	52.0 (44.0; 61.0)	
Age at graft collection (years)	55.4 ± 10.8	61.7 ± 5.6	53.6 ± 11.3	0.004*
	57 (49.0; 64.0)	62 (58.3; 67.3)	54.0 (47.0; 62.0)	
Age at blood sample (years)	58.6 ± 11.5	67.2 ± 6.2	56.2 ± 11.5	0.000*
	60.0 (51.0; 68.0)	68.5 (63.0; 71.0)	56.0 (49.0; 66.0)	
Sex (female/male; n = 81)	41/40	9/9	32/31	1.00
Cancer diagnosis (multiple myeloma/lymphoma/germ cell tumor; n = 81)	59/18/4	13/5/0	46/13/4	0.481
Regimen of high-dose chemotherapy before ASCT (high-dose melphalan/BEAM or other BCNU-based regimen/carboplatin and etoposide; n = 81)	58/18/5	13/5/0	45/13/5	0.417
Leukocytes[a] ($\times 10^3/mm^3$)	4.9 ± 3.5	3.8 ± 1.7	5.2 ± 3.8	0.130
	4.2 (3.1; 5.8) (n = 78)	3.6 (2.9; 4.6) (n = 18)	4.5 (3.4; 6.2) (n = 60)	
Neutrophils[a] ($\times 10^3/mm^3$)	2.6 ± 1.4	2.2 ± 1.5	2.7 ± 1.4	0.174
	2.3 (1.6; 3.4) (n = 77)	1.8 (1.5; 2.9) (n = 18)	2.5 (1.6; 3.5) (n = 59)	
Monocytes[a] ($\times 10^3/mm^3$)	0.5 ± 0.4	0.4 ± 0.2	0.6 ± 0.5	0.262
	0.5 (0.3; 0.6) (n = 77)	0.4 (0.3; 0.6) (n = 18)	0.5 (0.3; 0.6) (n = 59)	
Lymphocytes[a] ($\times 10^3/mm^3$)	1.2 ± 0.7	1.0 ± 0.6	1.2 ± 0.7	0.222
	1.0 (0.8; 1.5) (n = 77)	0.9 (0.7; 1.4) (n = 18)	1.0 (0.8; 1.6) (n = 59)	
Hemoglobin[a] (g/dL)	11.9 ± 1.9	11.8 ± 1.7	11.9 ± 2.0	0.944
	11.9 (10.9; 13.3) (n = 78)	11.9 (10.9; 13.4) (n = 18)	11.9 (10.8; 13.3) (n = 60)	
MCV[a] (fL)	91.8 ± 5.8	90.8 ± 4.9	92.1 ± 6.0	0.412
	91.1 (87.8; 95.0) (n = 78)	91.6 (86.6; 94.6) (n = 18)	90.7 (87.9; 95.6) (n = 60)	
RCDW[a] (%)	15.0 ± 2.3	16.2 ± 3.2	14.6 ± 1.9	0.009*
	14.6 (13.4; 15.4) (n = 78)	14.7 (14.4; 16.6) (n = 18)	14.3 (13.2; 15.3) (n = 60)	
Thrombocytes[a] ($\times 10^3/mm^3$)	153 ± 74	129 ± 74	160 ± 73	0.112
	159 (109; 202) (n = 78)	132 (58; 187) (n = 18)	160 (119; 206) (n = 60)	
CRP[a] (mg/dL)	1.69 ± 5.17	2.76 ± 8.45	1.37 ± 3.69	0.321
	0.28 (0.13; 0.99) (n = 77)	0.34 (0.15; 2.14) (n = 18)	0.28 (0.13; 0.9) (n = 59)	
Absolute number of collected CD34+ cells ($\times 10^6$)	835.0 ± 411.0	814.6 ± 476.6	840.7 ± 395.2	0.824
	776.0 (500.1; 1158.6) (n = 73)	620.8 (415.0; 1401.1) (n = 16)	857.4 (512.3; 1129.5) (n = 57)	
Number of collected CD34+ cells ($\times 10^6$/kg body weight)	11.2 ± 5.6	10.5 ± 6.8	11.4 ± 5.3	0.551
	10.2 (7.2; 15.1) (n = 73)	7.9 (6.0; 12.7) (n = 16)	10.4 (7.8; 15.3) (n = 57)	
Days as inpatient during first transplantation	19.0 ± 5.2	20.71 ± 6.06 (n = 17)	18.52 ± 4.90 (n = 62)	0.126
	17.0 (15.0; 22.0) (n = 79)			
Days to neutrophil engraftment[b] during first transplantation	7.0 ± 2.0	8.1 ± 2.9	6.7 ± 1.6	0.008*
	7.0 (6.0; 8.0) (n = 79)	7.0 (6.5; 9.0) (n = 17)	7.0 (5.0; 7.0) (n = 62)	
Hospitalization after first transplantation[c] (yes/no; n = 81)	48/33	12/6	36/27	0.590

(*Continued on next page*)

Table 1. *Continued*

Attribute	Total Cohort (n = 81)	CHIP Positive in Blood (n = 18)	CHIP Negative in Blood (n = 63)	p Value (CHIP Positive versus Negative)
Hospitalization in days/ follow-up year after transplantation[c]	8.67 ± 25.56	5.1 ± 6.9 3.4 (0; 8.4)	9.7 ± 28.7 2.0 (0; 7.9)	0.502
Cardiovascular events in patient history (yes/no; n = 81)	16/65	4/14	12/51	0.765
Death at last follow-up (yes/no; n = 81)	14/67	5/13	9/54	0.286
Progress of cancer at last follow-up (yes/no; n = 81)	38/43	12/6	26/37	0.067
Therapy with cytostatic agents before autologous transplantation (yes/no; n = 81)	72/9	15/3	57/6	0.408
Radiotherapy before blood sample (yes/no; n = 81)	29/52	6/12	23/40	1.00
Number of autologous transplantations before blood sample (1/2/3/4; n = 81)	51/22/7/1	13/4/1/0	38/18/6/1	0.786

Continuous variables are shown as mean ± SD; median (interquartile range). Categorical variables are shown as absolute numbers. BEAM, carmustine, etoposide, cytarabine, melphalan; BCNU, carmustine; MCV, mean corpuscular volume; RCDW, red cell distribution width; CRP, C-reactive protein. An asterisk (*) indicates significant p values ($p < 0.05$).

[a]Blood parameters at the time of the blood sample.

[b]First day of neutrophils below 500/mm^3 to the day before neutrophils above 500/mm^3.

[c]Excluding hospitalizations for prescheduled transplantation.

originate from the engrafted LT-HSCs and therefore retrospectively read out the potential of LT-HSCs (Benz et al., 2012). Reports investigated the presence of CHIP in the collected grafts of patients with lymphoid diseases undergoing ASCT (Gibson et al., 2017; Chitre et al., 2018) and showed reduced overall survival and a higher incidence of therapy-related myeloid neoplasms (t-MN) in patients carrying CHIP mutations in their pretransplant sample (Gibson et al., 2017). An analysis of the development of mutated clones by sequencing matched graft and post-transplantation samples was done either only in lymphoma patients who progressed into a t-MN (Gibson et al., 2017; Berger et al., 2018) or, in a single study, in 40 lymphoma patients in short-term follow-up of several months (Wong et al., 2018). In the latter study, most mutated clones remained stable in size after ASCT, and highly depending on the affected gene, only a small proportion increased in size (Wong et al., 2018). In our work, we aimed to study the development of non-malignant CHIP-mutated blood cell clones in 81 patients with myeloma, lymphoma, or solid tumors upon ASCT and cytotoxic therapy in a long-term clinical follow-up.

RESULTS

To investigate whether cytotoxic therapy and blood reconstitution-induced stress of HSCs in the setting of transplantation lead to increased frequency and outgrowth of CHIP-mutated cells, we sequenced the frozen stem cell graft (apheresis product), as well as several follow-up peripheral blood (PB) samples, of 81 patients who underwent ASCT for the treatment of myeloma (59 patients), lymphoma (18 patients), or germ cell tumors (4 patients) and were regularly examined in our outpatient clinic (Table 1). We explicitly excluded patients who developed a secondary myeloid malignancy to investigate non-malignant clonal development.

First, we analyzed the PB for mutations in 55 genes associated with CHIP and found that 18 of 81 patients (22%) were CHIP carriers with a variant allele frequency (VAF) of at least 2% (Figure 1A; Table S1). Twenty-eight non-synonymous mutations in 9 genes were identified, with DNMT3A, PPM1D, TET2, and TP53 as the most commonly affected genes (Figure 1B; Table S1). Of 18 CHIP-carrying patients, 9 patients harbored more than 1 mutation (8 patients with 2 mutations and 1 patient with 3 mutations), and 1 patient had a VAF above 50%, indicating loss of heterozygosity. The average VAF of all mutations in the blood samples was 10.7%.

There was no significant difference in hemoglobin levels or the distribution of PB cell lineages in CHIP-carrying patients in comparison to non-CHIP patients in follow-up PB analyses (Table 1). Furthermore, equal numbers of CD34+ cells were harvested after mobilization. The treatment of CHIP and non-CHIP carriers for their malignancies, including chemotherapy and/or radiation therapy, were similar. Patients with CHIP were significantly older

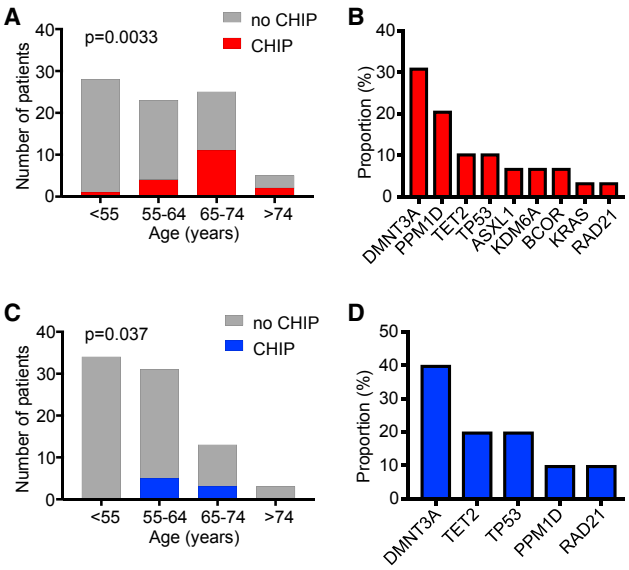

Figure 1. Incidence of CHIP and Prevalence of Mutated Genes after ASCT and in the Collected Graft

(A and C) Incidence of CHIP in 81 patients with a variant allele frequency (VAF) of at least 2% in peripheral blood samples after ASCT (A) and collected graft before ASCT (C), according to age group. The p value was calculated by a chi-square test.

(B and D) Prevalence of mutated genes in peripheral blood samples after ASCT (B) and collected graft before ASCT (D).

The list of analyzed genes and individual mutations is in Table S1.

at diagnosis of their malignant disease, at stem cell collection, and at first follow-up PB analysis than patients without CHIP, demonstrating, in line with other studies, that CHIP coincides with age (Table 1). However, the CHIP prevalence in our relatively young patient cohort (mean age of 59 years) was higher (22%) than expected from other cohorts analyzed with similar sensitive methods (Buscarlet et al., 2017; Arends et al., 2018). In particular, the observed high frequency of 44% of CHIP carriers post-transplantation in the age group of 65 to 74 years would be expected in patients who are at least 10 years older (Figure 1A).

Next, we sought to assess whether the existence of specific CHIP mutations could be tracked back to the graft, which had been collected, on average, 38 months (range of 1.5 to 169 months) before sampling of the post-transplantation PB or whether they developed after stem cell collection. To this end, we determined the CHIP status of the graft from our 81 patients by error-corrected deep amplicon sequencing, which allows detection of small clones down to a VAF of 0.5%. First, we screened for the presence of CHIP with a VAF threshold of at least 2%. We identified CHIP (VAF $\geq$ 2%) in 9 of 81 patients (11%) (Figure 1C), with 10 somatic mutations affecting 5 genes. DNMT3A and TET2 were the most prevalent genes in the grafts, representing 60% of cases, followed by TP53, PPM1D, and RAD21 (Figure 1D). The incidence of CHIP detected in the grafts of these patients was lower than determined in the same cohort after ASCT. The distribution of affected genes resembled the pattern of CHIP-associated mutations seen in hematologically normal patient cohorts (Buscarlet et al., 2017). Most importantly, 9 of the 10 mutations found in the graft were also detected in the matched follow-up PB. The VAF of these mutations increased in 7 of 8 patients from the graft (mean VAF of 11.8%) to the follow-up PB (mean VAF of 28.1%), with only 1 patient showing a slight decrease (graft, 4.8%; PB, 2.0%) (Figure 2A).

Furthermore, we searched for the presence of the remaining 19 mutations that appeared in the follow-up PB sample in their corresponding grafts by lowering the threshold of clonal detection to a VAF > 0.5% by error-corrected sequencing. Using this sensitive detection method, we found 7 of the 19 mutations at a low level already in the graft, showing an increase in mean VAF from 0.7% in the grafts to 6.4% in the post-transplant PB samples (Figure 2B). Twelve mutations with a mean post-transplantation VAF of 3.0% were not detectable in the matched grafts and were either below our detection threshold or had arisen after graft collection (Figure 2C).

Altogether, in 13 of 18 post-transplantation CHIP patients, 16 of 28 mutations identified in the follow-up PB samples could be traced back to the graft, and the clone size generally increased after transplantation (mean fold increase of 6.3 and range of 0.43- to 29.2-fold), with only 1 of 16 mutations showing a decrease (Figure S1). Thus, in most patients, mutations were not induced by high-dose chemotherapy administered before reinfusion of the graft but preexisted in the patient at the time of graft collection and conferred a reconstitution advantage to mutated HSCs in the setting of ASCT. In addition, new clones became detectable after ASCT (Figure 2C; Figure S1). Although we found a significant increase of VAFs from the graft to the first follow-up PB sample (Figure 3A), the VAFs remained relatively stable over time in the PB of individual patients (Figure 3B). Thus, the transplantation, not the time after transplantation, led to the pronounced increase in clonal burden. Furthermore, we showed by following CHIP development in individual patients, after two rounds of ASCT with aliquots of the same graft, that the ASCT conditioning regime largely eradicated the endogenous blood system and the blood reconstitution was largely dominated by the graft (Figure S2). The level of CHIP after secondary ASCT was returned to the status of the graft and subsequently increased again, reflecting the situation of CHIP development after primary ASCT (Figure S2). Although most patients in our cohort received cytotoxic therapy before the collection of the graft, we had 3 multiple myeloma patients out of 18 patients harboring CHIP after ASCT without pretransplantation chemotherapy. Unique patient number (UPN) 5 with a VAF of 4% in the follow-up sample was negative for the matched mutation in the graft. UPN14 harbored two mutations: one was not detectable in the graft, and the other one expanded 5.3-fold from low-level VAF in the graft to the follow-up sample. UPN16 had already detectable CHIP in the graft (VAF of 15%), and the clone expanded 2.6-fold after ASCT (to VAF of 40%). These cases only represent examples suggesting that CHIP accelerates by the hematopoietic stress induced by transplantation, independent of cytotoxic treatment before transplantation, which warrants validation in a larger cohort of patients.

Next, we assessed whether CHIP carriers have altered blood reconstitution by comparing the days in neutropenia after ASCT. As shown in Table 1, patients with CHIP require

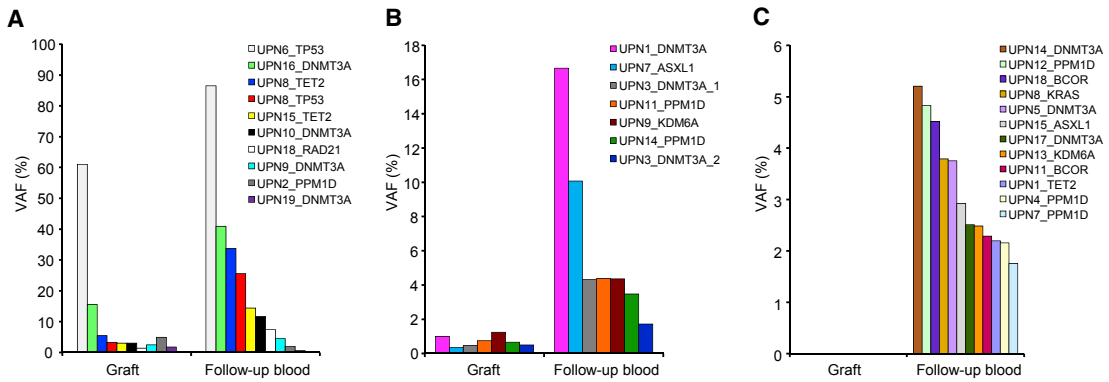

Figure 2. Development of Individual Mutated Clones after ASCT

(A–C) Individual clones with their VAF are shown in the collected graft before ASCT and in the corresponding follow-up peripheral blood sample after ASCT of (A) patients with CHIP (VAF $\geq$ 2%) in the graft, (B) CHIP-negative patients with detectable mutations (VAF < 2%) in the graft, and (C) patients with no detectable mutations in their graft (sensitivity of VAF $\geq$ 0.5%). Identical mutations (clones) have the same color in the graft and peripheral blood sample. UPN, unique patient number.

See also Figure S1.

significantly longer for neutrophil reconstitution. Multivariate regression analysis, including the age of the patients at graft collection, revealed that the presence of CHIP is an independent marker for the time in neutropenia after ASCT, with a hazard ratio (HR) of 2.77 (p = 0.002), whereas the patient age at ASCT did not remain significant.

We restricted our analyses to distinct subgroups of CHIP-driver genes, assembling DNMT3A, TET2, ASXL1, KDM6A, BCOR, and KRAS mutations as age-related gene mutations and mutations in PPM1D, TP53, and RAD21 as DNA-damage response genes. Patients with CHIP mutations exclusively in DNA-damage response genes showed the longest delay in neutrophil reconstitution (10.5 days for DNA-damage response CHIP, 7.38 days for age-related CHIP, and 6.66 days for non-CHIP; p = 0.001). A larger study of more patients undergoing ASCT is warranted to validate and delineate the clinical consequences of neutropenia in the context of certain CHIP-driver mutations.

Finally, we compared patients with CHIP (VAF $\geq$ 2%) already in their graft versus patients who never developed CHIP during the observation period. These patients with CHIP in their graft had a significantly longer period of hospitalization after ASCT (22.6 ± 6.0 versus 18.5 ± 4.9 days; p = 0.035) and a strong trend towards prolonged neutropenia (7.8 ± 0.9 versus 6.7 ± 1.6 days; p = 0.068) (Table S3).

DISCUSSION

We demonstrate here that recurrently found CHIP mutations are manifested in stem and progenitor cells with blood reconstitution

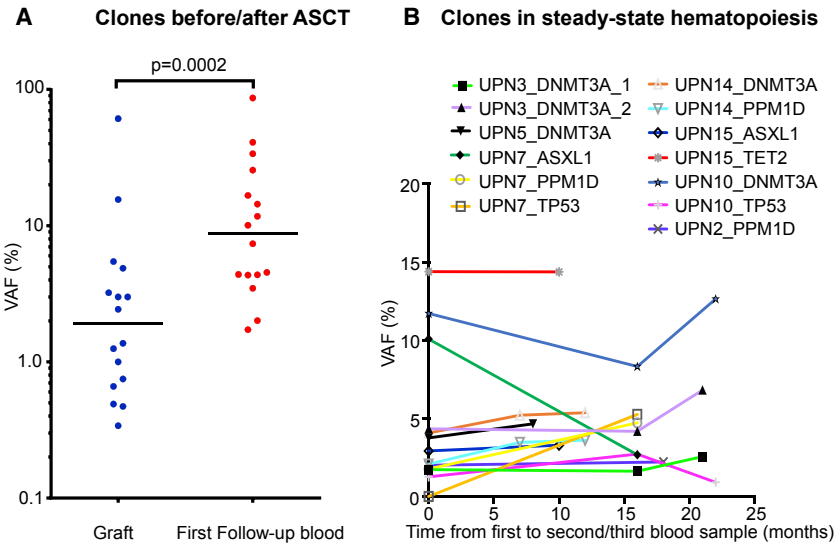

Figure 3. Comparison of Clonal Development after ASCT and in Steady-State Hematopoiesis

(A) VAFs for each detectable clone in the graft and in the first follow-up post-transplantation peripheral blood sample.

(B) Comparison of VAFs of the first available post-transplantation peripheral blood sample (time point 0) and additional follow-up blood samples of selected patients. Each symbol represents the VAF of one mutation of an individual patient (UPN) at different time points (months) after the first blood sample.

See also Figures S1 and S2.

capacity and that they confer enhanced capacity to dominate blood reconstitution over wild-type HSCs upon autologous transplantation. CHIP-mutated HSCs can be mobilized using standard agents, and they successfully engraft long term in the recipient upon ASCT, although with a longer hospitalization period. The ongoing treatment of the patients for their malignancies may have contributed to hematopoietic stress, promoting the expansion of CHIP-mutated clones, as previously shown for HSCs with PPM1D mutations (Hsu et al., 2018).

In homeostasis, clinically silent clonal hematopoiesis is detectable in almost all individuals by middle age (Young et al., 2016). However, these mutations conferred only a modest advantage (median VAF of 0.24%) and remained stable over 10 years. In contrast, we show that in almost all cases, the mutated clone increased in size, providing direct evidence that CHIP-mutated HSCs gain a clonal advantage upon hematopoietic stress. After reestablishing homeostasis, the expanded CHIP clones remained stable, suggesting that steady-state hematopoiesis relies predominantly on immature multipotent cells with previously underestimated self-renewal capacity and the HSC compartment is largely quiescent (Sun et al., 2014) (Busch et al., 2015). Therefore, stress on HSCs in people carrying CHIP might be detrimental to the accumulation of mutated blood cell lineages and their functional consequences. Lymphoma patients undergoing ASCT with a CHIP-mutated graft have a significantly inferior overall survival rate (Gibson et al., 2017). However, a study followed the VAF of CHIP-mutated blood cell clones in lymphoma patients 6- to 12-months after ASCT and found that most clones remained stable (Wong et al., 2018) and that the clonal development after ASCT largely depended on the mutated gene. While 20% of the DNMT3A-mutated clones increased on average 2-fold after ASCT, and more than 60% remained stable, most PPM1D-mutated clones decreased in size (Wong et al., 2018). These are striking differences to our findings. In our study, only two clones (mutations in PPM1D and DNMT3A) decreased in size after ASCT, while 22 clones increased by 6.7-fold on average, which may be explained by the longer observation time after ASCT, allowing hematopoiesis to return to the steady state, and by the nature and treatment of the lymphoid disease. In our case, most CHIP-positive patients suffered from multiple myeloma, not from lymphoma.

Larger studies are warranted to evaluate the clinical consequences of increasing clone sizes and individual genetic lesions after transplantation. Because the clone size correlates with the incidence of myeloid malignancies and cardiovascular diseases (Jaiswal et al., 2017), clinicians may consider monitoring CHIP status in the graft and after transplantation, especially in elderly patients. A study showed that allogeneic stem cell transplantation with a donor graft harboring CHIP seemed safe and resulted in a similar survival rate, albeit with a higher incidence of graft-versus-host disease (Frick et al., 2019).

Little is known about the functional consequences of most CHIP-related mutations on different blood cell lineages. Altered cytokine and chemokine profiles of myeloid cells may cause alterations in immune cell profiles in chronic cardiovascular diseases (Fuster et al., 2017; Jaiswal et al., 2017; Sano et al., 2018). These detrimental changes warrant further molecular and functional studies on the impact of distinct recurrent mutations on various blood cell lineages and on stem and progenitor cells for therapeutic interventions.

STAR★METHODS

Detailed methods are provided in the online version of this paper and include the following:

- KEY RESOURCES TABLE
- CONTACT FOR REAGENT AND RESOURCE SHARING
- EXPERIMENTAL MODEL AND SUBJECT DETAILS
  - Study Cohort
- METHOD DETAILS
  - Sample preparation for targeted sequencing
  - Targeted amplicon sequencing
  - Variant calling and annotation
- QUANTIFICATION AND STATISTICAL ANALYSIS
- DATA AND SOFTWARE AVAILABILITY

SUPPLEMENTAL INFORMATION

Supplemental Information can be found online at https://doi.org/10.1016/j.celrep.2019.04.064.

ACKNOWLEDGMENTS

We thank Kristina Götze and Stefanie Jordan for help with the UCT biobank and Stefanie Müller for providing the frozen grafts and data on graft collection. The study was supported in part by the German Research Foundation (SFB 834 project Z1 to L.D. and M.A.R. and project RI2462/1-1 to M.A.R.) and by the LOEWE Centers Cell and Gene Therapy Frankfurt (Hessisches Ministerium für Wissenschaft und Kunst, III L 4-518/17.004 [2014]) and Frankfurt Cancer Institute (Hessisches Ministerium für Wissenschaft und Kunst, III L 5-519/03/03.001 [0015]) to M.A.R. and C.A.O.

AUTHOR CONTRIBUTIONS

C.A.O. and M.A.R. wrote the manuscript, initiated and supervised the study, and interpreted the data. C.A.O., L.D., K.A.-E.-A., S.W., J.H., and T.S. performed and analyzed experiments. C.A.O., L.D., K.A.-E.-A., A.S., and J.H. established technologies and acquired data. S.W., K.A.-E.-A., and B.A. performed the bioinformatic data analyses. C.A.O., J.H., H.B., H.P., H.M., S.S., B.S., J.R., S.H., A.D., G.B., and C.H.B. contributed to the assembly of biological samples and clinical data. B.B., C.H.B., and H.S. supported and advised the study. All authors discussed early versions of the manuscript and provided comments and suggestions for change. All authors have approved the final manuscript for publication.

DECLARATION OF INTERESTS

All authors declare no competing interests.

Received: December 16, 2018
Revised: February 2, 2019
Accepted: April 12, 2019
Published: May 14, 2019

REFERENCES

Arends, C.M., Galan-Sousa, J., Hoyer, K., Chan, W., Jäger, M., Yoshida, K., Seemann, R., Noerenberg, D., Waldhueter, N., Fleischer-Notter, H., et al. (2018). Hematopoietic lineage distribution and evolutionary dynamics of clonal hematopoiesis. Leukemia *32*, 1908–1919.

Benz, C., Copley, M.R., Kent, D.G., Wohrer, S., Cortes, A., Aghaeepour, N., Ma, E., Mader, H., Rowe, K., Day, C., et al. (2012). Hematopoietic stem cell subtypes expand differentially during development and display distinct lymphopoietic programs. Cell Stem Cell *10*, 273–283.

Berger, G., Kroeze, L.I., Koorenhof-Scheele, T.N., de Graaf, A.O., Yoshida, K., Ueno, H., Shiraishi, Y., Miyano, S., van den Berg, E., Schepers, H., et al. (2018). Early detection and evolution of preleukemic clones in therapy-related myeloid neoplasms following autologous SCT. Blood *131*, 1846–1857.

Buscarlet, M., Provost, S., Zada, Y.F., Barhdadi, A., Bourgoin, V., Lépine, G., Mollica, L., Szuber, N., Dubé, M.-P., and Busque, L. (2017). *DNMT3A* and *TET2* dominate clonal hematopoiesis and demonstrate benign phenotypes and different genetic predispositions. Blood *130*, 753–762.

Busch, K., Klapproth, K., Barile, M., Flossdorf, M., Holland-Letz, T., Schlenner, S.M., Reth, M., Höfer, T., and Rodewald, H.-R. (2015). Fundamental properties of unperturbed haematopoiesis from stem cells *in vivo*. Nature *518*, 542–546.

Cabezas-Wallscheid, N., Buettner, F., Sommerkamp, P., Klimmeck, D., Ladel, L., Thalheimer, F.B., Pastor-Flores, D., Roma, L.P., Renders, S., Zeisberger, P., et al. (2017). Vitamin A-Retinoic Acid Signaling Regulates Hematopoietic Stem Cell Dormancy. Cell *169*, 807–823.

Chitre, S., Stölzel, F., Cuthill, K., Streetly, M., Graham, C., Dill, C., Mohamedali, A., Smith, A., Schetelig, J., Altmann, H., et al. (2018). Clonal hematopoiesis in patients with multiple myeloma undergoing autologous stem cell transplantation. Leukemia *32*, 2020–2024.

Cingolani, P., Platts, A., Wang, L., Coon, M., Nguyen, T., Wang, L., Land, S.J., Lu, X., and Ruden, D.M. (2012). A program for annotating and predicting the effects of single nucleotide polymorphisms, SnpEff: SNPs in the genome of Drosophila melanogaster strain w1118; iso-2; iso-3. Fly (Austin) *6*, 80–92.

Dorsheimer, L., Assmus, B., Rasper, T., Ortmann, C.A., Ecke, A., Abou-El-Ardat, K., Schmid, T., Brüne, B., Wagner, S., Serve, H., et al. (2019). Association of Mutations Contributing to Clonal Hematopoiesis With Prognosis in Chronic Ischemic Heart Failure. JAMA Cardiol. *4*, 25–33.

Eaves, C.J. (2015). Hematopoietic stem cells: concepts, definitions, and the new reality. Blood *125*, 2605–2613.

Frick, M., Chan, W., Arends, C.M., Hablesreiter, R., Halik, A., Heuser, M., Michonneau, D., Blau, O., Hoyer, K., Christen, F., et al. (2019). Role of Donor Clonal Hematopoiesis in Allogeneic Hematopoietic Stem-Cell Transplantation. J. Clin. Oncol. *37*, 375–385.

Fuster, J.J., MacLauchlan, S., Zuriaga, M.A., Polackal, M.N., Ostriker, A.C., Chakraborty, R., Wu, C.-L., Sano, S., Muralidharan, S., Rius, C., et al. (2017). Clonal hematopoiesis associated with TET2 deficiency accelerates atherosclerosis development in mice. Science *355*, 842–847.

Garrison, E., and Marth, G. (2012). Haplotype-based Variant Detection from Short-read Sequencing. arXiv, arXiv:1207.3907v2 [q-bioGN]. https://arxiv.org/abs/1207.3907v2.

Genovese, G., Kähler, A.K., Handsaker, R.E., Lindberg, J., Rose, S.A., Bakhoum, S.F., Chambert, K., Mick, E., Neale, B.M., Fromer, M., et al. (2014). Clonal hematopoiesis and blood-cancer risk inferred from blood DNA sequence. N. Engl. J. Med. *371*, 2477–2487.

Gibson, C.J., Lindsley, R.C., Tchekmedyian, V., Mar, B.G., Shi, J., Jaiswal, S., Bosworth, A., Francisco, L., He, J., Bansal, A., et al. (2017). Clonal Hematopoiesis Associated With Adverse Outcomes After Autologous Stem-Cell Transplantation for Lymphoma. J. Clin. Oncol. *35*, 1598–1605.

Gillis, N.K., Ball, M., Zhang, Q., Ma, Z., Zhao, Y., Yoder, S.J., Balasis, M.E., Mesa, T.E., Sallman, D.A., Lancet, J.E., et al. (2017). Clonal haemopoiesis and therapy-related myeloid malignancies in elderly patients: a proof-of-concept, case-control study. Lancet Oncol. *18*, 112–121.

Hsu, J.I., Dayaram, T., Tovy, A., De Braekeleer, E., Jeong, M., Wang, F., Zhang, J., Heffernan, T.P., Gera, S., Kovacs, J.J., et al. (2018). PPM1D Mutations Drive Clonal Hematopoiesis in Response to Cytotoxic Chemotherapy. Cell Stem Cell *23*, 700–713.

Jaiswal, S., Fontanillas, P., Flannick, J., Manning, A., Grauman, P.V., Mar, B.G., Lindsley, R.C., Mermel, C.H., Burtt, N., Chavez, A., et al. (2014). Age-related clonal hematopoiesis associated with adverse outcomes. N. Engl. J. Med. *371*, 2488–2498.

Jaiswal, S., Natarajan, P., Silver, A.J., Gibson, C.J., Bick, A.G., Shvartz, E., McConkey, M., Gupta, N., Gabriel, S., Ardissino, D., et al. (2017). Clonal Hematopoiesis and Risk of Atherosclerotic Cardiovascular Disease. N. Engl. J. Med. *377*, 111–121.

Li, H., and Durbin, R. (2009). Fast and accurate short read alignment with Burrows-Wheeler transform. Bioinformatics *25*, 1754–1760.

McKerrell, T., Park, N., Moreno, T., Grove, C.S., Ponstingl, H., Stephens, J., Crawley, C., Craig, J., Scott, M.A., Hodkinson, C., et al.; Understanding Society Scientific Group (2015). Leukemia-associated somatic mutations drive distinct patterns of age-related clonal hemopoiesis. Cell Rep. *10*, 1239–1245.

Pei, W., Feyerabend, T.B., Rössler, J., Wang, X., Postrach, D., Busch, K., Rode, I., Klapproth, K., Dietlein, N., Quedenau, C., et al. (2017). Polylox barcoding reveals haematopoietic stem cell fates realized *in vivo*. Nature *548*, 456–460.

Sano, S., Oshima, K., Wang, Y., MacLauchlan, S., Katanasaka, Y., Sano, M., Zuriaga, M.A., Yoshiyama, M., Goukassian, D., Cooper, M.A., et al. (2018). Tet2-Mediated Clonal Hematopoiesis Accelerates Heart Failure Through a Mechanism Involving the IL-1β/NLRP3 Inflammasome. J. Am. Coll. Cardiol. *71*, 875–886.

Smith, T., Heger, A., and Sudbery, I. (2017). UMI-tools: modeling sequencing errors in Unique Molecular Identifiers to improve quantification accuracy. Genome Res. *27*, 491–499.

Steensma, D.P., Bejar, R., Jaiswal, S., Lindsley, R.C., Sekeres, M.A., Hasserjian, R.P., and Ebert, B.L. (2015). Clonal hematopoiesis of indeterminate potential and its distinction from myelodysplastic syndromes. Blood *126*, 9–16.

Sun, J., Ramos, A., Chapman, B., Johnnidis, J.B., Le, L., Ho, Y.-J., Klein, A., Hofmann, O., and Camargo, F.D. (2014). Clonal dynamics of native haematopoiesis. Nature *514*, 322–327.

Takahashi, K., Wang, F., Kantarjian, H., Doss, D., Khanna, K., Thompson, E., Zhao, L., Patel, K., Neelapu, S., Gumbs, C., et al. (2017). Preleukaemic clonal haemopoiesis and risk of therapy-related myeloid neoplasms: a case-control study. Lancet Oncol. *18*, 100–111.

Walter, D., Lier, A., Geiselhart, A., Thalheimer, F.B., Huntscha, S., Sobotta, M.C., Moehrle, B., Brocks, D., Bayindir, I., Kaschutnig, P., et al. (2015). Exit from dormancy provokes DNA-damage-induced attrition in haematopoietic stem cells. Nature *520*, 549–552.

Wilson, A., Laurenti, E., Oser, G., van der Wath, R.C., Blanco-Bose, W., Jaworski, M., Offner, S., Dunant, C.F., Eshkind, L., Bockamp, E., et al. (2008). Hematopoietic stem cells reversibly switch from dormancy to self-renewal during homeostasis and repair. Cell *135*, 1118–1129.

Wingett, S.W., and Andrews, S. (2018). FastQ Screen: A tool for multi-genome mapping and quality control. F1000Res. *7*, 1338.

Wong, T.N., Miller, C.A., Jotte, M.R.M., Bagegni, N., Baty, J.D., Schmidt, A.P., Cashen, A.F., Duncavage, E.J., Helton, N.M., Fiala, M., et al. (2018). Cellular stressors contribute to the expansion of hematopoietic clones of varying leukemic potential. Nat. Commun. *9*, 455.

Xie, M., Lu, C., Wang, J., McLellan, M.D., Johnson, K.J., Wendl, M.C., McMichael, J.F., Schmidt, H.K., Yellapantula, V., Miller, C.A., et al. (2014). Age-related mutations associated with clonal hematopoietic expansion and malignancies. Nat. Med. *20*, 1472–1478.

Young, A.L., Challen, G.A., Birmann, B.M., and Druley, T.E. (2016). Clonal haematopoiesis harbouring AML-associated mutations is ubiquitous in healthy adults. Nat. Commun. *7*, 12484.

Yu, K.-R., Espinoza, D.A., Wu, C., Truitt, L., Shin, T.-H., Chen, S., Fan, X., Yabe, I.M., Panch, S., Hong, S.G., et al. (2018). The impact of aging on primate hematopoiesis as interrogated by clonal tracking. Blood *131*, 1195–1205.

STAR★METHODS

KEY RESOURCES TABLE

REAGENT or RESOURCE	SOURCE	IDENTIFIER
Biological Samples		
Peripheral blood and mobilized CD34+ apheresis (graft) of patients included in this study	Goethe University Hospital Frankfurt am Main	https://www.kgu.de
Critical Commercial Assays		
QIAamp DNA Mini Kit	QIAGEN	Cat# 51306
TruSight Myeloid Sequencing Panel	Illumina	Cat# FC-130-1010
Q5 Hot Start High-Fidelity 2x Master Mix	New England Biolabs	Cat# M0494X
Agencourt AMPure XP Beads	Beckman Coulter	Cat# A63881
TruSeq Custom Amplicon Low Input Kit	Illumina	Cat# FC134-2001
DNA 1000 Kit	Agilent Technologies	Cat# 5067-1504
PhiX Sequencing Control V3	Illumina	Cat# FC-110-3002
MiSeq V3 600-cycle Kit	Illumina	Cat# MS-102-3003
NextSeq 500/550 High Output v2 Kit	Illumina	Cat# FC 404-2004
NextSeq 500/550 Mid Output v2 Kit	Illumina	Cat# FC 404-2003
TruSeq® Custom Amplicon Index Kit	Illumina	Cat# FC-130-1003
Oligonucleotides		
Primers for targeted sequencing of PPM1D: see Table S1	This paper	N/A
Software and Algorithms		
FastQC v. 0.11.4	Wingett and Andrews, 2018	https://www.bioinformatics.babraham.ac.uk/projects/fastqc/
BWA-MEM v. 0.7.12	Li and Durbin, 2009	https://sourceforge.net/projects/bio-bwa/files/
FreeBayes v. 1.0.1	Garrison and Marth, 2012	https://github.com/ekg/freebayes
SnpEff and SnpSift v. 4.2	Cingolani et al., 2012	http://snpeff.sourceforge.net
UMI-tools software package v. 0.5.0	Smith et al., 2017	https://github.com/CGATOxford/UMI-tools
R programming language v. 3.3.1		https://cran.r-project.org/bin/
Catalog of Somatic Mutations in Cancer		https://cancer.sanger.ac.uk/cosmic
ClinVar		https://www.ncbi.nlm.nih.gov/clinvar

CONTACT FOR REAGENT AND RESOURCE SHARING

Further information and requests for resources and reagents should be directed to and will be fulfilled by the Lead Contact, Michael A. Rieger (m.rieger@em.uni-frankfurt.de).

EXPERIMENTAL MODEL AND SUBJECT DETAILS

Study Cohort

Clinical data and biological specimens (frozen mobilized blood stem cells and peripheral blood (PB) after transplantation) were collected from 81 patients who had undergone autologous stem cell transplantation (ASCT) for lymphoma, myeloma or germ cell tumors between May 2002 and July 2017 at the University Hospital of the Goethe University, Frankfurt/Main, Germany, between December 2015 and July 2017 with the help of the UCT biobank. Age, gender and other patient characteristics of our cohort are listed in Table 1.

Exclusion criteria were the presence of known myeloid disease, secondary myeloid neoplasms, prior allogeneic stem cell transplantation.

All patients provided written informed consent for participation in this study. The ethics review board of the Goethe University in Frankfurt, Germany, approved the protocols (project number SHN-06-2015). The study complies with the Declaration of Helsinki.

METHOD DETAILS

Sample preparation for targeted sequencing

DNA was isolated with QIAamp DNA Mini Kit (QIAGEN, Netherlands) from deep-frozen samples of grafts (collected by apheresis after mobilization) or from peripheral blood, which were isolated by Ficoll density-gradient centrifugation. The concentration of the extracted genomic DNA was determined using the Qubit dsDNA HS Assay Kit (Life Technologies, USA) on a Qubit Fluorometer (Life Technologies, USA). The cellular composition of the apheresis collected for ASCT and the follow-up peripheral blood samples were largely comparable in their percentage of leukocyte populations.

First, grafts and blood samples of the cohort were sequenced with the TruSight Myeloid Sequencing Panel (Illumina, USA) and with a custom-made assay covering the coding region of exon 6 of PPM1D (NM_003620; Table S2). The TruSight Myeloid Sequencing Panel was performed according to the manufacturer's instructions with 50 ng gDNA input. Amplification of three amplicons covering exon 6 of PPM1D was performed with Primers "PPM1D_ex6," reported in Table S2. All three amplicons of one patient were then pooled and the addition of the Illumina i7 and i5 adaptor sequences was performed with primers "Illumina" shown in Table S2. Both rounds of PCR (annealing temperature 60°C, 25 cycles) were run with a Q5 Hot Start High-Fidelity 2x Master Mix (New England BioLabs, USA) on a T100 Thermal Cycler (Bio-Rad Laboratories, USA). Library purification for the TruSight Myeloid Sequencing Panel and PPM1D was done with Agencourt AMPure XP Beads (Beckman Coulter, USA). Second, all samples (grafts and granulocytes) from patients who showed a variant (for filtering, see below) in either graft or granulocytes with a variant allele fraction (VAF) $\geq$ 0.02 (2%) were validated with a custom panel based on the Illumina TruSeq Custom Amplicon Low Input assay. The panel includes 594 amplicons in 56 genes (Table S1) commonly mutated in CHIP and myeloid malignancies and allowed improved identification of low allele frequency variants through a dual strand approach and addition of 6-bp unique molecular identifiers (UMI) in the target specific primers to enable error corrected sequencing.

Target enrichment was performed from 40 ng genomic DNA according to the instructions of the TruSeq Custom Amplicon Low Input Kit (Illumina, USA). The hybridization of the oligo pool to the target regions, the extension from the upstream oligo and the following ligation to the 5′ end of the downstream oligo was performed on a T100 Thermal Cycler (Bio-Rad Laboratories, USA). Amplification of the ligation products and addition of the Illumina i7 and i5 adaptor sequences was performed on a T100 Thermal Cycler (Bio-Rad Laboratories, USA). After purification, library quality and size distribution were assessed on a Bioanalyzer 2100 (Agilent Technologies, USA) using the DNA 1000 Kit. Bead-based library normalization was performed before pooling of the individual libraries.

Targeted amplicon sequencing

The PPM1D libraries were denatured according to Illumina's recommendations for MiSeq and 10% PhiX was spiked in (PhiX Sequencing Control V3, Illumina, San Diego, CA, USA) and sequenced on a MiSeq benchtop sequencer (Illumina, USA) using a 2x300 approach on a MiSeq V3 600-cycle kit. Demultiplexing and fastq file generation occurred on the system using the MiSeq Reporter (v.2.6.2). The remaining libraries were diluted and denatured according to the NextSeq System Denature and Dilute Libraries Guide (Illumina, USA) and 1% PhiX DNA was added. Sequencing of pooled libraries prepared with the TruSight Myeloid Sequencing Kit (Illumina, USA) and the TruSeq Custom Amplicon Low Input Kit (Illumina, USA) was performed using the NextSeq 500/550 High Output v2 kit (300 cycles) and the NextSeq 500/550 Mid Output v2 kit (300 cycles) (Illumina, USA), respectively, on a NextSeq 500 sequencer (Illumina, USA) according to the manufacturer's instructions. The sequencer was operated in a paired-end sequencing mode with 2 × 150 bp read length and 2 × 8 bp index read length. The BCL files were demultiplexed and converted to FASTQ files using the FASTQ Generation tool on BaseSpace (Illumina, USA). For the Custom TruSeq runs, the median coverage across all samples was 4216x before UMI family clustering and 391x with inclusion of UMIs. The median coverage for the TruSight Myeloid runs was 14572x.

Variant calling and annotation

For the PPM1D and TruSight Myeloid Panel libraries, read quality was assessed using FastQC (Wingett and Andrews, 2018). Subsequently, reads were mapped to the hg19 draft of the human genome using BWA-MEM (Li and Durbin, 2009). Variant calling was performed using FreeBayes (Garrison and Marth, 2012) with an allele frequency threshold of 0.02, a minimum alternate read count of 5 and a minimum base and mapping quality of 20. Variant effect prediction and variant annotation was performed using SnpEff and SnpSift (Cingolani et al., 2012). For the TruSeq Custom Amplicon Kit, FASTQ files from each patient were merged and reads were grouped into unique molecular identifier (UMI) families using the UMI-tools software package (Smith et al., 2017) before mapping to the draft of human genome. Afterward, the 'dedup' command of the UMI-tools software package was used to remove PCR duplicates with the same UMIs and alignment coordinates. Variant calling was performed as previously described, except that no allele frequency threshold was used and a minimum alternate read count of 2 given.

The identified variants were processed and filtered using the R programming language (ver. 3.3.1). Common SNPs with a minor allele frequency $\geq$ 5% in either the 1000 Genomes Project, Exome Variant Server or ExAC databases were excluded. In addition,

variants with a low mapping quality (< 20) and variants occurring in 8% or more of the subjects in the studied cohort were considered technical artifacts and excluded.

Furthermore, variants covered with less than 100 reads in the case of PPM1D and TruSight Myeloid Panel, variants with less than 100 reads in both sets of amplicons (CAT A or CAT B) or called in only one of the set of amplicons (CAT A or CAT B) in the case of the TruSeq Custom Panel, SNPs identified as common in the dbSNP database ($\geq$1% in the human population), and variants with sequence ontology terms ''LOW'' or ''MODIFIER'' (synonymous variant, 5′ UTR premature start codon gain variant; splice region variants, stop retained variant, 5′ UTR variant, 3′ UTR variant, non-coding exon variant, intron variant, non-coding transcript variant, upstream gene variant, downstream gene variant, intergenic variant, transcript variant, intragenic variant) were filtered out. All variants with a VAF $\geq$ 0.02 (2%) were considered, VAF was calculated by using the formula VAF = alternate reads / (reference + alternate reads). In the TruSeq Custom Panel, samples with a VAF $\geq$ 0.02 (2%) in either CAT A or CAT B were considered as CHIP positive and otherwise characterized as low level mutation. The comparison of the mutant allele quantification using both panels (TruSight+PPM1D and TruSeq) on identical samples from several patients revealed very similar VAFs (Pearson's correlation r^2 = 0.9886, $p < 0.0001$).

The variants were further validated on the basis of being reported in the literature and/or the Catalog of Somatic Mutations in Cancer (COSMIC; https://cancer.sanger.ac.uk/cosmic) and ClinVar (https://www.ncbi.nlm.nih.gov/clinvar).

QUANTIFICATION AND STATISTICAL ANALYSIS

Continuous variables are presented as mean ± standard deviation, unless otherwise noted. Analysis-of-variance (ANOVA) testing was used for comparison of continuous variables between groups. Categorical variables were compared with the chi-square test or Fisher's exact test, as appropriate. Statistical significance was assumed if $p < 0.05$, all reported p values are 2-sided. Statistical analysis was performed with SPSS (Version 23.0, SPSS Inc.).

DATA AND SOFTWARE AVAILABILITY

Due to issues related to patient confidentiality, raw data is not currently available for patient targeted exome sequencing data. If consent and approval are granted in the future, the raw data will be made available at that time.

Cell Reports, Volume *27*

Supplemental Information

Functional Dominance of CHIP-Mutated Hematopoietic Stem Cells in Patients Undergoing Autologous Transplantation

Christina A. Ortmann, Lena Dorsheimer, Khalil Abou-El-Ardat, Jennifer Hoffrichter, Birgit Assmus, Halvard Bonig, Anica Scholz, Heike Pfeifer, Hans Martin, Tobias Schmid, Bernhard Brüne, Sebastian Scheich, Björn Steffen, Julia Riemann, Stella Hermann, Alexandra Dukat, Gesine Bug, Christian H. Brandts, Sebastian Wagner, Hubert Serve, and Michael A. Rieger

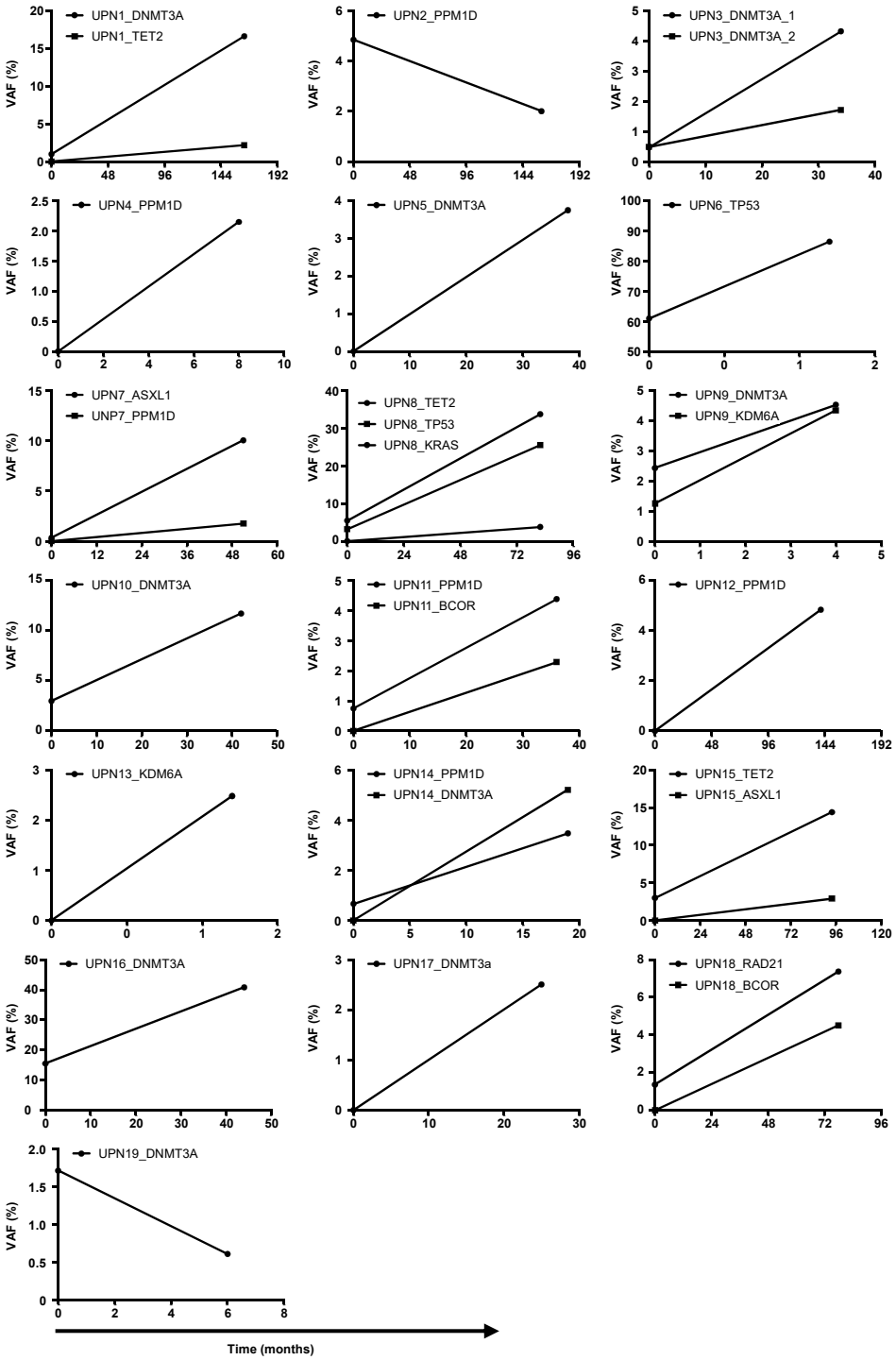

Figure S1. Comparison of variant allele frequencies (VAFs) of graft and first available peripheral blood sample. Related to Figures 2 and 3. Each graph represents one patient (UPN1-UPN19) and depicts one or multiple detected mutations and the time span between transplantation (at time point 0) and blood sample in months. UPN, unique patient number.

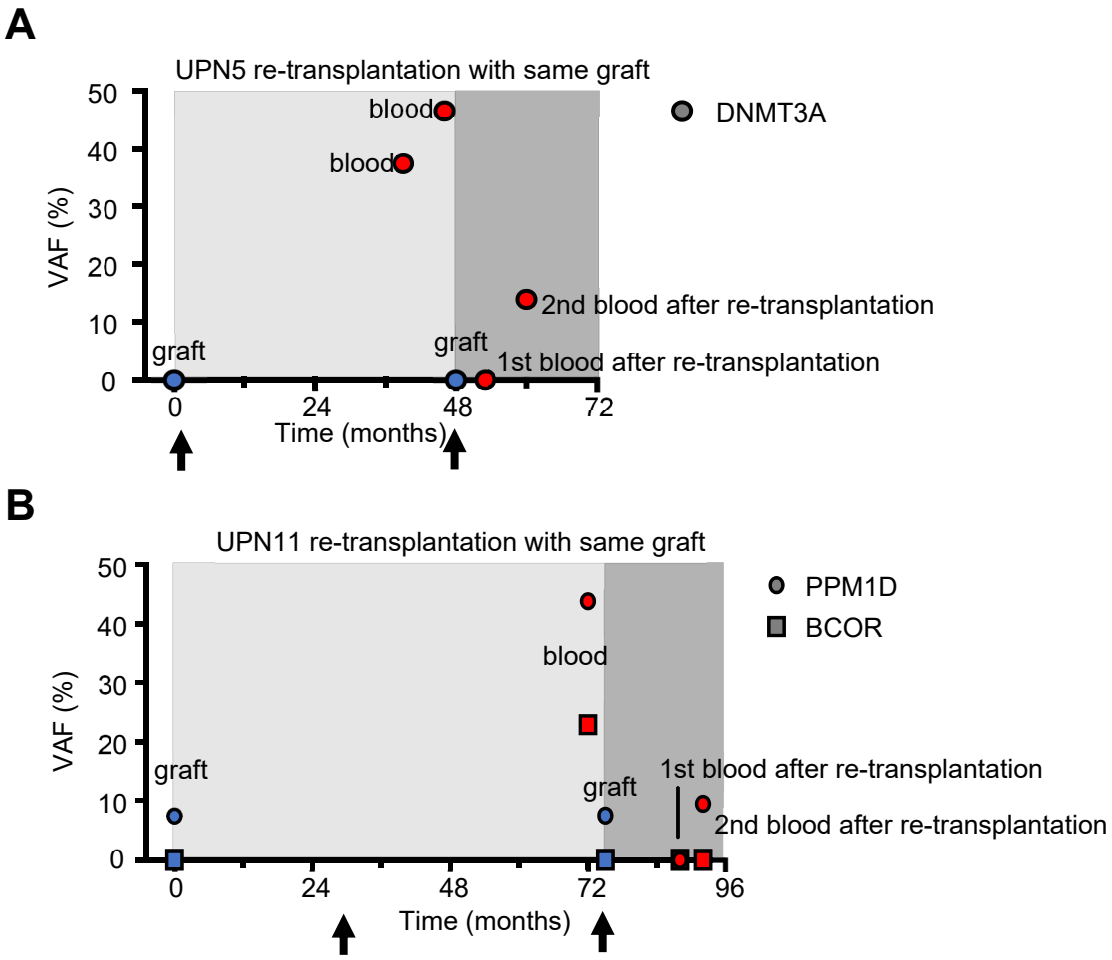

Figure S2. CHIP development of two patients undergoing a second transplantation. Related to Figures 3. Each graph shows the variant allele frequency (VAF) of the graft (DNMT3A mutation in patient UPN5 (A), PPM1D and BCOR mutation in patient UPN11 (B)), the post-transplantation blood sample(s) and blood samples taken after re-transplantation with the same graft. The time span after graft collection is shown on the x-axis. Arrows indicate ASCTs.

Table S3. Baseline characteristics of patient cohort according to CHIP status in collected graft. Related to Table 1.

Attribute	Total cohort (n=71)	CHIP positive in graft (n=9)	CHIP negative in graft and follow-up blood (n=62)	P-Value (CHIP positive versus negative)
Age at cancer diagnosis (years)	53.2±11.9 55.0 (47.0;63.0)	63.4±3.4 63.0 (60.0;67.0)	51.7±11.9 51.5 (44.0;61.0)	0.005*
Age at graft collection (years)	54.7±11.2 56.0 (48.0;64.0)	64.0±3.5 64.0 (60.5;67.5)	53.3±11.3 54.0 (47.0;62.0)	0.007*
Sex (female/male; n; n=71)	36/35	5/4	31/31	1.00
Therapy with cytostatic agents before autologous transplantation (yes/no; n; n=71)	64/7	8/1	56/6	1.00
Cancer diagnosis (multiple myeloma/lymphoma/germ cell tumor; n; n=71)	52/15/4	7/2/0	45/13/4	0.735
Days as inpatient during first transplantation	19.0±5.2 17.0 (15.0;21.5) (n=69)	22.6±6.0 22.5 (16.5;28.5) (n=8)	18.5±4.9 17.00 (15.0;20.0) (n=61)	0.035*
Days to neutrophil engraftment[a] during first transplantation	6.8±1.6 7.0 (5.5;7.5) (n=69)	7.8±0.9 7.5 (7.0;8.8) (n=8)	6.7±1.6 7.0 (5.0;7.0) (n=61)	0.068
Hospitalization in days/follow-up year after transplantation[b]	9.3±27.2 2.0 (0;7.9)	5.2±9.1 0.3 (0;7.3)	9.9±28.9 2.1 (0;8.0)	0.635
Hospitalization after first transplantation[b] (yes/no; n; n=71)	41/30	5/4	36/26	1.00
Absolute number of collected CD34+ cells ($x10^6$)	825.8±284.9 812.3 (514.4;1101.0) (n=63)	666.4±284.9 284.9 (517.0;776.0) (n=7)	846.5±396.4 865.5 (511.3;1143.8) (n=56)	0.235
Number of collected CD34+ cells ($x10^6$/ kg bodyweight)	11.2±5.2 10.3 (7.5;15.2) (n=63)	8.9±4.1 7.5 (6.3;12.1) (n=7)	11.5±5.3 10.5 (7.8; 15.3) (n=56)	0.209
Death at last follow-up (yes/no; n; n=71)	12/59	3/6	9/53	0.172
Progress of cancer at last follow-up (yes/no; n; n=71)	32/39	6/3	26/36	0.282

Continuous variables are shown as mean ± standard deviation; median (interquartile range), categorical variables are shown as absolute numbers. An asterisk (∗) indicates significant p values ($p < 0.05$).

[a] First day of neutrophils below 500 /mm^3 to day before neutrophils over 500/mm^3.

[b] Excluding hospitalizations for prescheduled transplantation.